Land-cover Mapping in the Brazilian Amazon Using SPOT-4 Vegetation Data and Machine Learning Classification Methods

João M.B. Carreiras, José M.C. Pereira, and Yosio E. Shimabukuro

Abstract

The main objective of this study is to evaluate the feasibility of deriving a land-cover map of the state of Mato Grosso, Brazil, for the year 2000, using data from the 1 km SPOT-4 VEGETATION (VGT) sensor. For this purpose we used a VGT temporal series of 12 monthly composite images, which were further transformed to physical-meaningful fraction images of vegetation, soil, and shade. Classification of fraction images was implemented using several recent machine learning developments, namely, filtering input training data and probability bagging in a classification tree approach.

A 10-fold cross validation accuracy assessment indicates that filtering and probability bagging are effective at increasing overall and class-specific accuracy. Overall accuracy and mean probability of class membership were 0.88 and 0.80, respectively. The map of probability of class membership indicates that the larger errors are associated with cerrado *savanna and semi-deciduous forest.*

Introduction

The importance of tropical forests (e.g., the Amazon forest) and the surrounding environment has been increasing, as specific threats and problems (e.g., deforestation, timber logging, infrastructure development, and mining) are generating increased atmospheric carbon dioxide concentration, with severe present and future consequences in climate (Batjes and Sombroek, 1997; Vitousek *et al.*, 1997; Houghton, 2000; Schulze *et al.*, 2003). The Amazon forest is a unique ecosystem, driven by its moist climate and is home to hundreds of thousands of animal and plant species (Goulding *et al.*, 2003). It is also important to consider the areas of cerrado savanna and seasonal forest, where deforestation has been as intense as in areas of moist forest (Fearnside, 1993; Miranda *et al.*, 1996; Nepstad *et al.*, 1997; Kaimowitz and Smith, 2001). In the past thirty to forty years, the Amazon forest has suffered several aggressions that led to deforestation of large areas of native forest for agricultural and pasture uses, as well as for mining and timber activities (Moran *et al.*, 1994; Nepstad *et al.*, 1997). Integrated satellite and census data showed that part of the state of Mato Grosso within the hydrological borders of the Amazon and Tocantins rivers has experienced a 50 percent increase in total agricultural area between 1980 (approximately 94,115 km^2) and 1995 (approximately 140,845 km^2), due to duplication in cropland (soybean and sugar cane plantations) and triplication of planted pasture, at the expense of natural pasture (Cardille and Foley, 2003). Estimates based on manual interpretation of high-resolution satellite imagery, produced by the Brazil's National Space Research Institute (INPE), indicate that in the state of Mato Grosso (Brazil), deforestation in areas of moist and seasonal forest reached a value of 143,930 km^2 by the end of the year 2000, which is close to 25 percent of the total area deforested in the Brazilian Legal Amazon (INPE, 2002). The Mato Grosso State Foundation for the Environment (FEMA-MT), using manual interpretation of high-resolution satellite data, estimated that deforestation in this state reached a value of 270,283 km^2 by the end of 1999 (SEPLAN, 2002). The difference between INPE's and FEMA-MT's estimates is mostly due to the deforestation in areas of *cerrado* savanna, considered by the later. However, a state-level licensing and enforcement program for clearing by large farmers and ranchers, implemented by the FEMA-MT since 1999, appears to become effective at controlling deforestation, with the observed decreased of deforestation rate between 1999 and 2000 (Fearnside, 2003; Fearnside and Barbosa, 2003). These dynamics make Mato Grosso one of the most rapidly changing states within the Brazilian Legal Amazon. Considering the unique characteristics of the Amazon forest and its interfaces with other important vegetation types, this state is representative of the moist forest, *cerrado* savanna and seasonal forest, their diverse interfaces, and underlying changes. Up-to-date, accurate maps of land-cover and land-use are required for monitoring the impacts on the carbon and water cycle, biotic diversity, and soil degradation (Houghton *et al.*, 2000 and 2001; Lambin *et al.*, 2003).

The need for timely and accurate environmental information have driven the development of new optical sensors, e.g., the Moderate Resolution Imaging Spectroradiometer (MODIS), the VEGETATION (VGT), and the Advanced Along Track Scanning Radiometer (AATSR) sensors, onboard the Terra/Aqua, SPOT-4, and ENVISAT satellites, respectively, and stimulated the improvement of methods for land-cover mapping (Friedl *et al.*, 2002; Eva *et al.*, 2004). These sensors were partially designed for land applications, either to

João M.B. Carreiras and José M.C. Pereira are with the Department of Forestry, Instituto Superior de Agronomia, Tapada da Ajuda, 1349-017 Lisboa, Portugal (jmbcarreiras@isa.utl.pt; jmcpereira@isa.utl.pt).

Yosio E. Shimabukuro is with the Remote Sensing Department, Instituto Nacional de Pesquisas Espaciais, Av. dos Astronautas, 1758, CEP 12227-010, São José dos Campos, SP, Bazil (yosio@ltid.inpe.br).

Photogrammetric Engineering & Remote Sensing
Vol. 72, No. 8, August 2006, pp. 897–910.

0099-1112/06/7208–0897/$3.00/0

provide accurate and operational measurements of simple characteristics of vegetation canopies, and qualitative land-cover information. The data, with enhanced spectral, spatial, radiometric, and geometric quality, and acquired on a daily basis, have the potential for land-cover change monitoring, especially in these tropical regions where cloud coverage is high. The use of coarse optical remote sensing imagery has proven to be a valuable tool to map and monitor land-cover changes from regional to global scales (Hansen *et al.*, 2000; Achard *et al.*, 2001; Friedl *et al.*, 2002; Eva *et al.*, 2004). Hansen *et al.* (2000) produced a 1 km, 12-class global land-cover map (i.e., the University of Maryland global land-cover map), using 1992–1993 data from the Advanced Very High Resolution Radiometer (AVHRR). Achard *et al.* (2001), in the scope of the TRopical Ecosystem Environment observation by Satellite (TREES) project, mapped several land-cover classes over the pan-tropical humid forest belt, using early 1990's AVHRR data. Friedl *et al.* (2002) produced a 1 km, 17-class global land-cover map (i.e., the Boston University global land-cover map), updated at quarterly (96 day) intervals, using Terra/Aqua MODIS data. Eva *et al.* (2004) produced a 1 km, 42-class vegetation map of South America for the year 2000, as part of the Global Land-Cover 2000 (GLC2000) project, using four sets of satellite information: Along Track Scanning Radiometer (ATSR-2) onboard the ERS-2 satellite, SPOT-4 VGT, JERS-1 radar data, and the Defense Meteorological Satellite Program (DMSP) Operational Linescan System (OLS).

Land-cover classification from remote sensing data has relied on parametric classifiers (distributional assumptions), such as supervised quadratic discriminant analysis (QDA) (i.e., maximum likelihood classifier) or unsupervised clustering methods (Richards, 1986; Lillesand and Kiefer, 1994). Machine learning techniques, such as decision trees, neural networks, and *k*-nearest neighbors classifiers have been applied to land-cover classification at global, continental, and regional scales (DeFries *et al.*, 1998; Friedl *et al.*, 1999; Hansen *et al.*, 2000; Franco-Lopez *et al.*, 2001; Friedl *et al.*, 2002; Brown de Colstoun *et al.*, 2003). Decision trees, developed by Breiman *et al.* (1984) as classification and regression trees (CART), require no distributional assumptions, can handle data represented on different measurement scales, yield a set of explicit rules which are easy to interpret, can handle missing data, and produce a variable importance score. Some refinements have been introduced to basic decision tree algorithms, namely the notion of ensemble (or committee) of classifiers. Bagging (bootstrap aggregation) (Breiman, 1996) and boosting (Freund and Schapire, 1996) are methods that generate committees of classifiers, and combine them by simple or weighted voting from the individual classifiers (Breiman, 1998). These methods have proven to be very successful in improving the classification accuracy of decision tree classifiers (Mclin and Opitz, 1997; Bauer and Kohavi, 1998; DeFries and Chan, 2000). In land-cover mapping the possibility of obtaining estimates of probability of class membership is also important. Recently, Provost and Domingos (2003), using learning-curve analysis, showed that simple modifications to tree induction algorithms (e.g., CART, C4.5) can produce better probability estimates, especially when rankings based on probability of class membership are required. Furthermore, they concluded that probability bagging is successful in improving probability estimates in several real world datasets, even more than it improves classification accuracy. Friedman *et al.* (2000) have demonstrated boosting as being equivalent to additive logistic regression. Therefore, using boosting in association with a classification algorithm (e.g., CART), probabilities of class membership (or confidence) can be assigned to each class at every pixel (McIver and Friedl, 2001; Friedl *et al.*, 2002;). Furthermore, McIver and Friedl (2001) tested this approach using three different datasets and demonstrated that incorrectly classified pixels tend to have low classification confidence, while correctly classified pixels tend to have higher confidence. Another important development has been the use of classification algorithms to identify mislabeled training observations, that can occur for several reasons, including subjectivity, data-entry error, or inadequacy of the information used to label each observation (John, 1995; Brodley and Friedl, 1999). The filtered training set is then used as input to the final classification algorithm, thus resulting in a classifier with increasing classification accuracy (John, 1995; Brodley and Friedl, 1996; Brown de Colstoun *et al.*, 2003). The filtering procedure is more important if the final classification algorithm has a tendency to be fit to errors and/or outliers, as is the case of boosting (Brodley and Friedl, 1999).

The main objective of this study is to assess the adequacy of a temporal series of monthly composite images of the SPOT-4 VGT sensor to produce a land-cover map of the state of Mato Grosso for the year 2000. The dataset used is the first yearly temporal series of daily 1 km spatial resolution optical satellite imagery for the Amazon region. Several studies have demonstrated that land-cover classification can be achieved more accurately using a multitemporal dataset that represents the phenological variability of vegetation (Friedl *et al.*, 1999; Brown de Colstoun *et al.*, 2003). In this study, we also evaluated the importance of identifying mislabelled training data and probability bagging as methods to improve classification accuracy and probability-based rankings of class membership.

Study Area and Legend Definition

The state of Mato Grosso is located in the western-central part of Brazil, at 06° to 19° South and 50° to 62° West (Figure 1), and has an area of 903,358 km^2 (IBGE, 2000). At the end of the 1980s, federal and state governments proposed to the World Bank the Program of Agro-environmental Development (PRODEAGRO), which, in turn, requested the elaboration of an Agro-ecological Zoning of Mato Grosso. Therefore, a 39-class vegetation map (PRODEAGRO) was produced, basically derived from the 1:250 000 scale RADAMBRASIL mapping (Brazil, 1980, 1982a, and 1982b), but represented at a scale of 1:1 500 000. The RADAMBRASIL project (between 1973 to 1983) intended to represent the spatial distribution of potential vegetation types, i.e., without anthropic influence. For ease of representation and description of the main land-cover types of Mato Grosso, we aggregated it into a 4-class map. The main vegetation types are ombrophyllous forest, seasonal forest, *cerrado* savanna, and water (Fearnside and Barbosa, 2003) (Figure 1). The climate is humid in the northern part of the state (maximum of two months of dry season), becoming less humid in the central and south part of the state, where the dry season is longer (Velloso *et al.*, 1974). Nevertheless, it is common to consider that the dry season lasts from May to September, while the wet season goes from October to April. The ombrophyllous forest is related with the humid climate of the northern part of the state. The seasonal forest and *cerrado* savanna are associated with the less humid areas of central and south Mato Grosso, respectively. Currently, most of the deforested areas are under pasture or agricultural use or, to a lesser extent, left abandoned, permitting the regeneration of secondary forest (Moran, 1993; Fearnside, 2003).

The legend used in this study was derived with the Land-cover Classification System (LCCS) of the Food and Agriculture Organization (FAO) of the United Nations (Di Gregorio and Jansen, 2000). It is a standardized classification

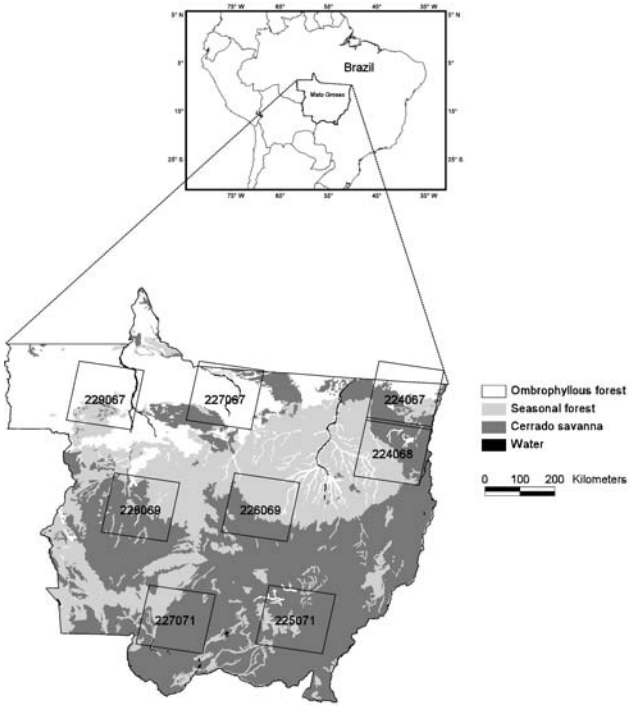

Figure 1. The state of Mato Grosso, Brazil, respective insertion in South America, and main vegetation types, as defined by the PRODEAGRO vegetation map. It is also shown the location of the eight Landsat 5 TM and Landsat 7 ETM+ scenes used for identification of areas of known land-cover.

system for the definition of land-cover classes, which uses a combination of independent hierarchically arranged diagnostic criteria. In Mato Grosso, we have defined a 9-class legend, according to FAO-LCCS principles. The correspondence between this legend and the 39-class PRODEAGRO vegetation map is shown in Table 1.

The broadleaved evergreen forest (BEF) class corresponds, in general, to the ombrophyllous forest, characterized by tall evergreen trees occurring in tropical areas without a strong biologic dry period (less than 60 days) (Goulding *et al.*, 2003). The semi-evergreen forest (SEF) class refers to a combination of dominant broadleaved evergreen vegetation and with broadleaved deciduous vegetation covering more than 25 percent (Di Gregorio and Jansen, 2000). The semi-deciduous forest (SDF) class is comparable to the previous class, though referring to a combination of broadleaved deciduous vegetation that is dominant and with broadleaved evergreen vegetation representing more than 25 percent tree cover (Di Gregorio and Jansen, 2000). The two previous classes define the so-called seasonal forest, occurring in areas characterized by two distinct seasons. The following four classes represent distinct types of *cerrado* savanna, ranging from open grassland (*campo limpo*) to closed-canopy forest (*cerradão*) (Miranda *et al.*, 1996). The broadleaved evergreen woodland (BEW) class can either be considered as open-canopy arboreal woodland or as closed canopy forest (*cerradão*) (Miranda *et al.*, 1996). The broadleaved evergreen sparse trees (BEST) and broadleaved evergreen shrubland (BES) classes are characterized by a closed (*cerrado sensu stricto*) or open (*campo cerrado*) scrub, respectively, both of which may have scattered trees (Miranda *et al.*, 1996). The open grassland (OG) class is dominated by C_4 grasses without woody vegetation (*campo limpo*), or including a few scattered shrubs (*campo sujo*) (Miranda *et al.*, 1996). The herbaceous crops (HC) class is used here as a proxy for areas that were cleared of its original vegetation cover in the past, and that presently are under agricultural or pasture use.

Data

The original data used in this study was a set of daily 1 km SPOT-4 VGT images spanning the whole of year 2000 and covering the entire state of Mato Grosso, Brazil (1345 $\times$ 1267 pixels) (images from days of the year 39, 45, 58, 77, 134, 178, 213, 220, 230, 252, 280, 292, and 294 were not available or had unrecoverable errors). We used the S1 product, consisting of 1 km georeferenced, calibrated, atmospherically corrected surface reflectance data (Passot, 2000). Among other characteristics, the VGT sensor onboard the SPOT-4 and SPOT-5 satellites provides a better imagery acquisition geometry and additional reflective bands [blue 0.43 to 0.47 μm, red 0.61 to 0.68 μm, near infrared (NIR) 0.78 to 0.89 μm, and short wave infrared (SWIR) 1.58 to 1.75 μm], when compared with the formerly used AVHRR (Hansen *et al.*, 2000; Achard *et al.*,2001), which only has the red band (0.58 to 0.68 μm) and the NIR band (0.72 to 1.10 μm) in the reflective part of the electromagnetic spectrum.

We combined the SPOT-4 VGT S1 daily images into 12-monthly composite images. Each monthly composite image was produced by combining a monthly compositing criterion and a transformation of principal components analysis, with the objective of minimizing cloud cover, while preserving as much as possible the original spatial structure of the data. The monthly compositing algorithm uses different criteria according to the nature of the land-cover, as defined by a vegetation index, in this case the Soil Adjusted Vegetation Index (SAVI) (Huete, 1988). If a pixel is considered to represent a vegetated surface (SAVI above a given threshold) then a date

TABLE 1. LEGEND USED IN THIS STUDY, DERIVED FROM FAO/LCCS (DI GREGORIO AND JENSEN, 2000), RESPECTIVE ACRONYMS, AND CORRESPONDING PRODEAGRO CLASSES

FAO/LCCS Classes (this study)	Legend Acronyms	PRODEAGRO Classes
Broadleaved evergreen forest	BEF	As, As1, As3, Da, Ds, Ds1, ON, Paa, Pab, Pah
Semi-evergreen forest	SEF	Fa, Fa2, Fb, Fs, Fs2, Fs3, TN
Semi-deciduous forest	SDF	Cb5, Cs, Cs2, Cs3
Broadleaved Evergreen Woodland	BEW	Sd, Sd1, Sd2
Broadleaved Evergreen Sparse Trees	BEST	Sa, Sa1, Sa2
Broadleaved Evergreen Shrubland	BES	SN, Sp1, Sp2, Sp4, Spf, Sps
Open Grassland	OG	Sg2, Sg4, Sgf, Sgs, Tg4
Herbaceous Crop(s)	HC	Not mapped
Natural/Artificial Waterbodies	NAW	Water

TABLE 2. ORIGINAL AND FILTERED TRAINING DATASET, DISCRIMINATING THE NUMBER OF TRAINING PIXELS AND TRAINING SITES PER LAND-COVER CLASS, BEFORE AND AFTER THE APPLICATION OF CONSENSUS FILTERING IN A CLASSIFICATION TREE APPROACH

FAO/LCCS Classes	Before Filtering		After Filtering		Variation (%)
	# Pixels	# Sites	# Pixels	# Sites	
Broadleaved evergreen forest	640	160	626	158	2.2
Semi-evergreen forest	840	210	829	210	1.3
Semi-deciduous forest	120	30	102	29	15.0
Broadleaved Evergreen Woodland	160	40	129	39	19.4
Broadleaved Evergreen Sparse Trees	560	140	537	138	4.1
Broadleaved Evergreen Shrubland	400	100	384	100	4.0
Open Grassland	120	30	97	27	19.2
Herbaceous Crop(s)	1960	490	1933	487	1.4
Natural/Artificial Water Bodies	110	40	110	40	0.0
Total	4910	1240	4747	1228	3.3

of a minimum value of the SWIR band is selected, otherwise (SAVI below the threshold), indicating a bare ground/sparsely vegetated pixel, a minimum value of the red band is selected. Visual inspection and comparison of several SAVI thresholds indicated that a cut-off value of 0.3 was effective at separating vegetated from non-vegetated or sparsely vegetated areas. Furthermore, the Maximum Noise Fraction (MNF) transformation (Green *et al.*, 1988) was applied to the multitemporal dataset of monthly composite images and used as a method of additional signal-to-noise ratio improvement. The back-transformed dataset using the first i^{th} MNF eigenimages yielded an accurate reconstruction of monthly composite images from the dry season (May through September) and enhanced spatial coherence from wet season images (October through April). Detailed information about the compositing algorithm can be found in Carreiras and Pereira (2005).

Identification of areas of known land-cover in VGT data for image classification was carried out with the help of several ancillary datasets. The available 39-class PRODEAGRO vegetation map was used to select areas of homogeneous land-cover types, which were further refined by visual inspection of seven Landsat Thematic Mapper (TM)/Enhanced TM Plus (ETM+) scenes from 2000 and one Landsat ETM+ scene from 2001 (Figure 1). World Reference System (WRS) scenes 224/067, 224/068, 226/069, 227/067, and 227/068 were obtained from INPE, in the scope of the Prodes Digital Project (INPE, 2005), and scenes 225/071, 227/071, and 229/067 from the Global Land Cover Facility (GLCF), University of Maryland (UMD), U.S. (University of Maryland, 2005). Each training site (i.e., a group of adjacent pixels of the same class) was not allowed to exceed four pixels, and was selected far apart enough to minimize spatial-autocorrelation problems (Congalton, 1988; Friedl *et al.*, 2000; Muchoney and Strahler, 2002). The original training dataset is described in Table 2.

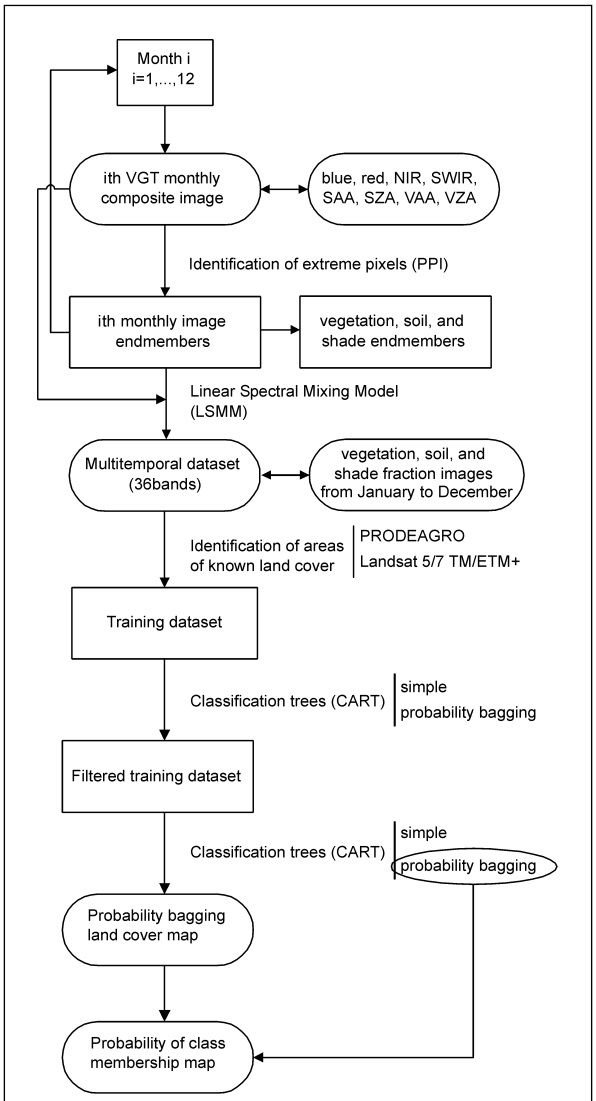

Figure 2. Flowchart outlining the steps used to produce the land-cover map and subsequent accuracy assessment.

Methods

In the literature (e.g., Hansen *et al.*, 2000; Friedl *et al.*, 2002; Eva *et al.*, 2004), common procedures for producing a land-cover map, from remote sensing data, include a first step of image processing (e.g., temporal compositing, image transformation), followed by the application of a specific classification algorithm to derive a land-cover map, and finally by map accuracy assessment. The main steps of the methodology used in this work are described below and summarized in Figure 2.

Linear Spectral Mixing Model

At a spatial resolution of 1 km, it is common for image pixels to correspond to a ground area occupied by more than one pure component or land-cover element (endmember), thus resulting in a mixed pixel (Adams *et al.*, 1986; Quarmby *et al.*, 1992). This is a consequence of the heterogeneity of ground cover and of the sensor spatial resolution, which is

often lower than that of the elements of interest (Chang and Heinz, 2000). The radiation received by an optical remote sensing system includes the signal of different pure elements, affected by atmospheric effects, which combine to produce a response with characteristics of the different components and their fractions (Shimabukuro and Smith, 1991).

Several studies have addressed the question of sub-pixel target detection in the Amazon region, using high- and low-resolution satellite imagery (Cross *et al.*, 1991; Holben and Shimabukuro, 1993; Adams *et al.*, 1995; Cochrane and Souza Jr, 1998; Souza Jr. *et al.*, 2003; Lu *et al.*, 2003). In the present study, we used a Linear Spectral Mixing Model (LSMM) to derive the fraction of pure elements present in each pixel. Although spectral mixing is not strictly linear, due to multiple scattering between elements, these models have generally yielded acceptable results (Oleson *et al.*, 1995). Fractions of endmembers are easier to interpret than spectral reflectances (Aguiar *et al.*, 1999), and, therefore, provide a more intuitively association between image measurements and observations in the field (Adams *et al.*, 1995). The correct application of this model is based on two assumptions (Adams *et al.*, 1986): (a) the multispectral imaging instrument should have a linear response with respect to reflectances, and (b) the number of endmembers should be less than the input dimensionality (i.e., smaller or equal than the number of spectral bands). The unconstrained option of this model was used, i.e., the sum of the fractions is not required to equal one, but allowing each pixel to assume any fraction value, either negative or super-positive (i.e., over one). Therefore, the reflectance of a pixel in each spectral band is expressed as a linear combination of the characteristic reflectances of its component endmembers, weighted by their respective areal fractions within the pixel (Ichoku and Karnieli, 1996). Equation 1 is the mathematic expression of the LSMM used in this study:

$$r_i = \sum a_{ij} \cdot x_j + \varepsilon_i \quad (1)$$

where r_i is the surface reflectance of an image pixel in band i, x_j the fraction of pure component (endmember) j, a_{ij} is the jth image endmember response for each band i, also in surface reflectance units, and ε_i the error term for band i (Shimabukuro and Smith, 1991). A measure of the error produced by the application of the LSMM in each pixel is given by the mean error (ME) (Equation 2):

$$ME = \sum |\varepsilon_i| / m \quad (2)$$

where m is the number of spectral bands used in the unmixing process. Another helpful measure of model fitting is the presence/absence of excessive negative and/or super-positive fraction values. The presence of such fraction values indicates an incorrect selection of endmembers. Consequently, it is an indication that the model was incorrectly fitted, and new endmembers need to be selected.

Using information from different studies in the same region (Holben and Shimabukuro, 1993; Rodríguez-Yi *et al.*, 2000; Carreiras *et al.*, 2002), and our own interpretation of the VGT satellite imagery, three endmembers were defined: vegetation, soil, and shade. Fractions of vegetation and soil are easily understandable, representing the proportion of vegetation and soil found within each pixel. The shade fraction is meant to represent shadowing due to vegetation structure, but is spectrally very similar to topographic shadows and water bodies. Consequently, it was postulated that all mixed pixels could be modelled with these three endmembers. Selection of pure endmembers in each VGT monthly composite image was accomplished through the Pixel Purity Index (PPI™) algorithm (Research Systems, Inc., 2000). The PPI™ is computed by repeatedly projecting n-dimensional scatterplots onto a random unit vector, according to a given number of iterations (Boardman *et al.*, 1995): 500 in our case. The extreme pixels in each projection are recorded and the total number of times each pixel is marked as extreme is kept (Research Systems, Inc., 2000). This extremity score can be shown to be related to pixel purity, using a convex geometry argument (Boardman, 1993). Then, a PPI™ image for each month was produced, with each pixel having a value corresponding to the number of times it was considered extreme (the maximum allowed was 500, i.e., the number of iterations). Afterwards, those extreme pixels were plotted in a red-NIR scatterplot, and the most pure endmembers were selected. The *greenest* pixel of vegetation (low red reflectance, high NIR reflectance), the *brightest* pixel of soil (high red reflectance, high NIR reflectance) and the *darkest* pixel of shade (reflectance close to zero in all spectral bands) were to be chosen among those several extreme pixels, per month. An example of endmember selection for the month of June is shown in Figure 3. At a spatial resolution of 1 km, it is almost impossible to find a pure pixel of shade, therefore for the application of LSMM it is acceptable to use water as a proxy for shade endmember (Shimabukuro and Smith, 1995). It was also assumed that a temporal variation in the fraction of vegetation, soil or shade could be associated with a change in the phenology of a vegetated land-cover type.

The application of LSMM to each monthly composite image was evaluated using three criteria: (a) presence of image fractions with significant numbers of negative or super-positive values, (b) analysis of ME histograms, and (c) correlation of vegetation fractions with a vegetation index (SAVI) calculated from the original spectral bands. Although variations in selected endmembers affect estimates of fractions, classification results were shown to be relatively insensitive to small variations in the endmembers (Adams *et al.*, 1995).

Classification Trees

Classification trees have previously been applied to land-cover classification from satellite data (DeFries *et al.*, 1998; Hansen *et al.*, 2000; Friedl *et al.*, 2002; Brown de Colstoun *et al.*, 2003). They are a classification procedure that recursively partitions a dataset into smaller homogeneous subsets using a set of condition rules (if . . . , then . . .) defined to split each parental node (Breiman *et al.*, 1984). Each tree is composed of a root node, containing all the training data,

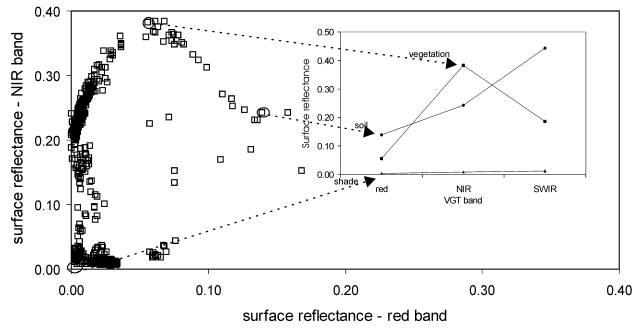

Figure 3. Scatterplot of extreme pixels selected by the PPI™ technique for the monthly composite image of June 2000, and indication of the selected vegetation, soil, and shade endmembers.

which is split into several intermediate nodes, and a set of terminal nodes. In univariate classification trees, such as those used in this study, each node is formed by a binary split of the parental node. Some advantages over traditional parametric classification methods include the non-parametric nature of the classifier, quantification of variable importance, disclosure of non-linear and hierarchical relationships between predictor variables, and allowance for missing values (Breiman *et al.*, 1984; Hansen *et al.*, 1996; Friedl and Brodley, 1997). In this study, we used the CART algorithm (Breiman *et al.*, 1984). According to Breiman *et al.* (1984), three fundamental steps are required to construct a classification tree: (a) the selection of a node splitting rule, (b) the decision whether to set a node as terminal or to continue splitting (stopping rule), and (c) the assignment of each terminal node to a given class of the response variable.

The splitting rule criterion has the goal of reducing the data variability in intermediate node split into two descendant nodes that are *purer* (Safavian and Landgrebe, 1991). Breiman *et al.* (1984) refer that one method of achieving this purpose is the definition of an impurity function *i(t)* at every intermediate node *t*, i.e., a measure of the heterogeneity of a given node. Consider that there is a candidate split rule *S* that divides an intermediate node *t* into left descendant node t_L and right descendant node t_R, such that a proportion p_L of the cases in *t* goes into t_L and a proportion p_R goes into t_R. Then, a measure of the goodness of the split *S* can be the decrease in intermediate node impurity, i.e., Equation 3:

$$\Delta i(S,t) = i(t) - i(t_L)p_L - i(t_R)p_R \quad (3)$$

Therefore, Breiman *et al.* (1984) refer that the selection of a optimal split *S* should minimize $\Delta i(S,t)$ over all possible splits *S*, i.e., the split that produces the maximum decrease in the node impurity. Breiman *et al.* (1984) refer several impurity functions, namely the Gini index and the Twoing criterion. The Gini index is more used in 2-class classification problems, and the Twoing criterion where the number of classes is higher (Breiman *et al.*, 1984). Accordingly, in this study we have used the Twoing criterion to estimate splits at each internal node of the tree.

A classification tree resulting from this procedure can be grown until all terminal nodes are pure. This leads to very large trees that may overfit the data, and is mainly due to the presence of noise in the training data (DeFries and Chan, 2000). Therefore, in order to choose a right sized tree, one must define a pruning rule, i.e., an approach for removing terminal and intermediate nodes. The CART pruning rule is based on a cost-complexity measure (Breiman *et al.*, 1984). This measure incorporates the resubstitution estimate of the true overall misclassification rate, the number of terminal nodes, and a complexity parameter (Breiman *et al.*, 1984). By using the resubstitution estimate the largest tree would be selected. Therefore, it must be estimated by means of a test set that is independent of the training set. This requires that the number of available observations be large enough to draw a test sample, otherwise the estimate can be obtained through *v*-fold cross validation (Bruno *et al.*, 2004). The objective is to select a less complex subtree (smaller number of terminal nodes), while minimizing the increase in misclassification error (Bell, 1996). In this study we used a 10-fold cross validation approach to assess the accuracy of the resulting classification trees. For this purpose, the original training dataset was randomly split into ten equal mutually exclusive subsets. For each subset (1/10), a tree is grown from the remaining subsets (9/10) and a subtree sequence obtained; the held out set (1/10) is then used to evaluate the sequence; this process is repeated ten times (Bell, 1996). In remote sensing imagery there is always some kind of spatial autocorrelation, i.e., neighboring observations are more spectrally similar than distant pixels (Congalton, 1988). Thus, enforcement of spatial separation of the mutually exclusive subsets is required, as failure to impose this condition can result in spuriously inflated classification accuracies (e.g., Friedl *et al.*, 2000). This was achieved by randomly selecting training sites (and not training pixels) for each one of the 10 mutually exclusive subsets. This approach will assure that pixels belonging to the same training site are selected either for growing the tree or for their evaluation, thus avoiding within-site spatial autocorrelation from affecting the results (McIver and Friedl, 2001; Muchoney and Strahler, 2002). Overall accuracy, omission and commission errors for each selected classification tree are provided (Congalton, 1991).

The easiest criterion for class assignment to each terminal node is basically a majority rule, i.e., the class that has most observations is assigned to that terminal node (Safavian and Landgrebe, 1991). However, this procedure can be influenced by error costs associated with misclassification errors in each class, and by previous knowledge of prevalence of each class of the response variable (Breiman *et al.*, 1984). Different combinations of these parameters will influence class assignment and misclassification error. In our study, we used available information from the PRODEAGRO vegetation map and estimates of deforestation from INPE and FEMA-MT to assign each land-cover class a prior probability. It has been shown that incorporating this information in a classification tree approach can improve classification results (e.g., McIver and Friedl, 2002). CART produces a measure of the importance of each predictor variable in the selected classification tree, giving important information about which months and/or fractions are more important for land-cover discrimination.

Identification of Mislabeled Training Data

Usually, training data contains mislabeled observations, either from incorrect data-entry, insufficient ancillary information, or subjectivity in the selection of representative observations. Recently, methods have been proposed to identify mislabeled training observations, as a way to improve classification results (John, 1995; Brodley and Friedl, 1999). Brodley and Friedl (1999) suggest using learning algorithms (e.g., classification trees, neural networks) to identify mislabeled data, serving as a filter for the final classification algorithm. They verified that consensus filtering (i.e., considering an observation as mislabeled only if all the algorithms failed to correctly classify it) is preferable when training data are not abundant. In this study we used a classification tree approach to mark each training observation as correctly or incorrectly labeled. For this purpose, the training data were randomly separated into 10 mutually exclusive sets. In each 9/10 we extracted 10 bootstrap samples and use it to build 10 classification trees. Only those observations in the remaining 1/10 incorrectly classified by all 10 trees are marked as mislabeled. This approach is conservative at throwing away good data, which might just be difficult to classify (Brodley and Friedl, 1999). After 10 iterations all the training data has been marked. Afterwards, only the observations in the filtered training dataset are used in the final classification algorithm.

Bagging and Probability of Class Membership

Some classification methods (e.g., classification trees and neural nets) are unstable, in the sense that they are affected by small perturbations in the training set, possibly originating large changes in the constructed classifiers (Breiman, 1996). Therefore, these unstable methods can have their accuracy improved by perturbing and combining, that is, generating

TABLE 3. LEGEND CORRESPONDENCE AMONG THIS STUDY, THE UMD (HANSEN *ET AL.*, 2000), BU (FRIEDL *ET AL.*, 2002), AND SA-GLC2000 (EVA *ET AL.*, 2004) LAND-COVER MAPS

This Study Legend	UMD Legend	BU Legend (UMD class scheme)	SA-GLC2000 Legend (level 2)
BEF+SEF+SDF	Everg. broad. forests, Decid. broad. forests	Everg. broad. forests, Decid. Broad. forests	Everg. broad. forests, Decid. forests, Semi-decid. forests
BEW	Woodlands	Woody savannas	Savanna
BEST	Wooded grasslands	Savannas	Shrub savannas
BES	Closed shrublands, Open shrublands	Closed shrublands, Open shrublands	Shrublands, Flooded shrubland
OG	Grasslands	Grasslands	Grasslands
HC	Croplands	Croplands	Agriculture-intensive, Mosaic degraded vegetation, Mosaic degraded forests
NAW	Water bodies	Water bodies	Natural and artificial water bodies

multiple versions of the classifier (i.e., ensembles, or committees) by perturbing the training set, then combining these multiple versions into a single predictor (Breiman, 1998). Methods that use ensembles of classifiers have demonstrated to be very successful in improving the accuracy of classification trees (Maclin and Opitz, 1997; Bauer and Kohavi, 1998). These methods can be divided in two types: those that adaptively change the distribution of the training set based on the performance of previous classifiers (e.g., boosting) and those that do not (e.g., bagging) (Bauer and Kohavi, 1998). The simplicity and success of bagging in improving classification accuracy compared with standard classification trees (e.g., DeFries and Chang, 2000) lead us to choose bagging as the approach to generate an ensemble classification tree.

In bagging, each sub-classifier c_i ($i = 1 \ldots n$) (in our case a classification tree) is run on n different b_i bootstrap samples of the original m training set observations. Each b_i is generated by uniformly sampling m observations from the training set with replacement. The final classifier c is built from c_i whose output is the class predicted most often by its sub-classifiers, with ties broken arbitrarily (Bauer and Kohavi, 1998). Although the main purpose of bagging is to build strong classifiers by means of variance reduction (Breiman, 1996), some variants of bagging have proven also to be adequate for the estimation of class membership probability (Breiman, 1996; Bauer and Kohavi, 1998; Perlich *et al.*, 2003; Provost and Domingos, 2003). Probability bagging is one such variants, so that instead of returning a classification, each sub-classifier returns a probability distribution for the classes in each terminal node (Provost and Domingos, 2003). Subsequently, the probability bagging algorithm averages the probability for each class over all sub-classifiers, and predicts the class with the highest probability. However, Provost and Domingos (2003) remark that these probability estimates of class membership serve only the purpose of ranking observations. We used 25 bootstrap replicates to build a probability bagging classification tree, evaluated with a 10-fold cross validation approach. Breiman (1996) suggests that a higher number of replicates tend not to produce a significant error decrease.

Accuracy Assessment

Commonly, a land-cover classification procedure ends with accuracy assessment of the resulting map. Traditional methods of accuracy assessment of thematic maps include comparison of maps with independent ground data, each ground point being assigned to a certain class and compared with the one on the map, resulting in a match or mismatch (Congalton, 2001; Foody, 2002). The difficulty in obtaining up-to-date independent information of spatial distribution of land-cover classes in the state of Mato Grosso led us to choose an alternative approach. The traditional confusion matrix (Congalton, 1991), constructed using the results from the 10-fold cross-validation, is used as a first approximation for overall and class-specific accuracies. The use of probability bagging classification tree provides information on probability-based rankings of class membership (Provost and Domingos, 2003). Therefore, the application of the probability bagging classifier to the whole state of Mato Grosso results in a map of probability-based rankings of class membership. These probability estimates of class membership are compared with class-specific accuracies, and used to extend and complete traditional accuracy assessment. McIver and Friedl (2001) and Friedl *et al.* (2002) used a similar approach, based on a recent development explaining boosting as a form of additive logistic regression (Friedman *et al.*, 2000), to build maps of classification confidence using a boosting algorithm and tree induction in several remote sensing datasets.

A more qualitative comparison with existing land-cover maps is performed, by assessing class overall extent in Mato Grosso. For that purpose, we compare the overall class extent resulting from this study with the University of Maryland (UMD) 1 km global land-cover map built with 1992 to 1993 AVHRR data (Hansen *et al.*, 2000). The same assessment is made with the Boston University (BU) 1 km global land-cover map obtained with 2001 MODIS data (Friedl *et al.*, 2002), and with the GLC2000 project (SA-GLC2000) 1 km South America land-cover map constructed with 2000 VGT data (Eva *et al.*, 2004). The BEF, SEF, and SDF classes were aggregated (BSS class), as some of the land-cover maps analyzed does not provide this level of discrimination. Table 3 provides the legend correspondence between this study and the three quoted land-cover maps.

Results and Discussion

LSMM Analysis

The performance of the application of the LSMM to VGT monthly composite images was evaluated using the ME, correlation of vegetation fractions with a vegetation index (SAVI), and evaluation of percentage of all pixels with endmember fractions between zero and one (Table 4). Mean ME is always below two percent and corresponding standard deviation does not exceed one percent, indicative of good performance of the LSMM used. Correlation of monthly vegetation fractions with monthly SAVI is high, indicating that vegetation fractions represent the abundance of vegetation per pixel. In February, October, November, and December

TABLE 4. MEASURES USED TO ASSESS THE APPLICATION OF LSMM TO VGT MONTHLY COMPOSITE IMAGES. MEAN AND STANDARD DEVIATION (IN PARENTHESES) ME ARE IN SURFACE REFLECTANCE UNITS

Month	Mean ME	Correlation Between Vegetation Fraction with SAVI	Proportion of Fraction Images with Values Between 0 and 1		
			Vegetation	Soil	Shade
January	0.016 (0.007)	0.875	0.999	0.999	0.943
February	0.016 (0.005)	0.829	0.993	0.999	0.091
March	0.009 (0.003)	0.864	0.999	0.999	0.964
April	0.006 (0.002)	0.904	0.994	0.996	0.979
May	0.006 (0.003)	0.947	0.989	0.995	0.999
June	0.009 (0.003)	0.974	0.999	0.852	0.999
July	0.009 (0.005)	0.981	0.962	0.710	0.999
August	0.014 (0.007)	0.970	0.960	0.708	0.998
September	0.012 (0.007)	0.984	0.992	0.924	0.966
October	0.016 (0.009)	0.979	0.994	0.999	0.860
November	0.016 (0.003)	0.970	0.973	0.895	0.691
December	0.011 (0.007)	0.937	0.997	0.999	0.369

the proportion of shade fraction images with pixels outside the zero to one interval is high. In October and November that proportion is made up of small negative shade fraction values, most of them less than 1 percent. In February and December negative shade fraction values were well above 1 percent. As the corresponding vegetation and soil fractions do not have significant values above one or below zero, we decided to keep these months in the dataset. The same applies for soil fractions in July and August. The easily interpretable splitting rules of classification trees combined with variable importance score give more insight about the importance of these variables for land cover prediction. Although there is always some error in LSMM analysis, physically-meaningful fraction images provide information that is more easily interpretable. As an example of the application of the LSMM model, the vegetation, soil, and shade fraction images for June 2000 are shown (Figure 4). In general, a shade fraction image represents canopy structure. The HC class usually have low proportion of shade fraction, as areas of bare soil, pasture, agriculture, and initial stages of regeneration have a short, homogeneous cover, causing little or no shadowing. Higher values of soil fraction (brighter white) can indicate also agriculture after harvesting, and intermediate values (light grey) are areas of *cerrado* savanna. BEF, SEF, and SDF classes are highlighted mainly by high values of vegetation fraction and low amount of soil fraction. As postulated, areas of NAW are associated with the highest values of shade fraction, due to spectral similarity.

Data Filtering and Classification

Overall, the approach for identifying mislabelled training data resulted in the removal of 3.3 percent of the original training data (Table 2). The classes with the greater number of mislabelled observations were BEW (19.4 percent), OG (19.2 percent), and SDF (15.0 percent). The remaining classes had few observations removed, always below five percent of the original data. The nature of the filter used, consensus filtering with 10 bootstrap samples, suggests that only mislabelled observations were removed. Observations that are just difficult to classify should be kept by this procedure, as suggested by Brodley and Friedl (1999). Only incorrectly classified observations by all the 10 sub-classifiers were marked as mislabelled.

Application of classification trees to the training dataset was done to assess the effect of identifying mislabelled training data (filtering) and probability bagging in classification accuracy. Consequently, four combinations were created: unfiltered training dataset with simple classification tree, unfiltered training dataset with probability bagging classification tree, filtered training dataset with simple classification

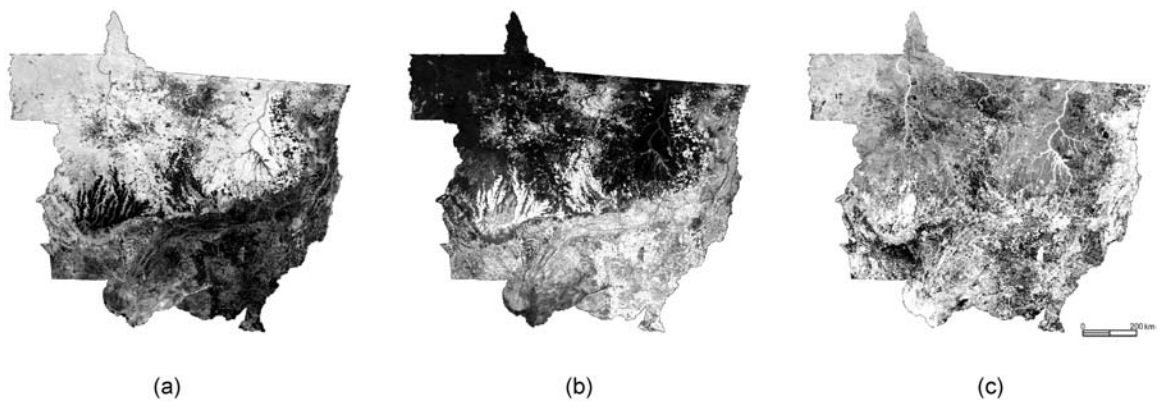

Figure 4. Fractions images of (a) vegetation, (b) soil, and (c) shade endmembers for July 2000, for the state of Mato Grosso, Brazil.

TABLE 5. COMPARISON OF CLASS-SPECIFIC ERRORS AND OVERALL ACCURACIES RESULTING FROM A 10-FOLD CROSS VALIDATION APPROACH OF UNFILTERED TRAINING SET WITH SIMPLE CLASSIFICATION TREE (UCT), UNFILTERED TRAINING SET WITH PROBABILITY BAGGING CLASSIFICATION TREE (UPB), FILTERED TRAINING SET WITH SIMPLE CLASSIFICATION TREE (FCT), AND FILTERED TRAINING SET WITH PROBABILITY BAGGING CLASSIFICATION TREE (FPB)

	Commission Error (%)				Omission Error (%)				Overall Accuracy			
Classes	UCT	UPB	FCT	FPB	UCT	UPB	FCT	FPB	UCT	UPB	FCT	FPB
BEF	22.5	15.1	16.0	13.7	15.9	12.0	13.1	9.1				
SEF	17.9	12.4	12.3	9.4	13.1	9.8	9.8	8.7				
SDF	47.2	37.5	42.0	28.6	84.2	54.2	60.8	51.0				
BEW	51.5	48.2	49.6	42.4	69.4	63.1	55.8	58.9				
BEST	45.2	36.2	38.3	31.9	18.6	25.2	18.6	21.4	0.81	0.85	0.85	0.88
BES	18.1	27.3	19.8	23.2	42.5	28.0	36.7	25.8				
OG	55.0	39.7	36.8	29.3	70.0	60.8	50.5	45.4				
HC	3.1	3.0	1.9	2.1	6.6	4.1	4.8	3.1				
NAW	2.8	0.9	0.0	0.0	5.5	0.9	8.2	0.9				

tree, and filtered training dataset with probability bagging classification tree. All of them were assessed using a 10-fold cross validation approach (Table 5).

The effect of filtering over simple classification trees resulted in a decrease in commission and omission errors, and in a relative gain of 4.94 percent in overall accuracy; the exceptions are the BES and NAW classes, which display small increases in commission and omission errors, respectively. The effect of filtering over probability bagging classification trees resulted in the decrease of commission and omission errors, and in a relative gain of 3.53 percent in overall accuracy. The effect of probability bagging in unfiltered training data is also the decrease of commission and omission errors, and a relative gain of 4.94 percent in overall accuracy; the exceptions are BES and BEST, with increased commission and omission errors, respectively. A reduction in commission and omission errors is also the effect of using probability bagging over filtered training data, with a relative gain of 3.53 percent in overall accuracy; the exceptions are BES and NAW with a little increase in commission error, and BEST and BEW with a small increase in omission error. These results shows that the combined application of filtering and probability bagging resulted in a general decrease in commission and omission errors, and in a relative increase of 8.64 percent in overall accuracy, from 0.81 to 0.88; the exceptions are BES and BEST, which has small increases in commission and omission errors, respectively. Nevertheless, the classifier built with filtered training set and probability bagging still produces several high class-specific errors (above 30 percent), especially commission errors in BEST and BEW classes, and omission errors in OG, SDF, and BEW classes. The high commission and omission error of BEW is the result of misclassified observations from the BEST class, a spectrally similar class of *cerrado* savanna (Table 6). The same pattern is observed for the other class with high commission error, BEST, which also result from confusion with spectral-nearby *cerrado* savanna classes. The high omission error of the SDF class results from observations misclassified as BEF and SEF, which are very similar to SDF, differing only in the proportion of deciduous tree cover. Also, the high omission error of the OG class results from observations misclassified as spectrally similar BEST, BES, and BEW *cerrado* savanna classes. These results indicates that SPOT VGT data has limitations in discriminating SDF from BEF and SEF classes, and in discriminating among the four *cerrado* savanna classes. This is a consequence of mapping a vegetation continuum assuming a *crisp* logic, in opposition to a fuzzy logic (Foody, 1999). This is partly overcome with probability bagging classification trees, by providing information about the probability of class membership.

The most important variables for predicting land-cover classes in the final filtered probability bagging classifier were obtained by averaging the contribution of each one in the 25 individual classification trees (Figure 5). The most important variables are the soil fractions from dry season months (May to September), and vegetation fractions of July and August. Conversely, shade fractions are less important and more scattered throughout the year. Dry season imagery appears to be are more important for discrimination of land-cover classes in the state of Mato Grosso than wet season data.

TABLE 6. CONFUSION MATRIX FOR THE 10-FOLD CROSS VALIDATION APPROACH USED TO ASSESS THE PROBABILITY BAGGING CLASSIFICATION TREE CONSTRUCTED WITH FILTERED DATA. OVERALL ACCURACY IS 0.88

	Predicted Class (# pixels)										
Observed Class (# pixels)	BEF	SEF	SDF	BEW	BEST	BES	OG	HC	NAW	Total	Omission Error (%)
BEF	569	47	10	0	0	0	0	0	0	626	9.1
SEF	61	757	9	0	1	0	1	0	0	829	8.7
SDF	25	20	50	1	3	0	2	1	0	102	51.0
BEW	0	6	0	53	63	1	3	3	0	129	58.9
BEST	0	0	0	29	422	54	11	21	0	537	21.4
BES	0	0	0	1	82	285	2	14	0	384	25.8
OG	1	4	1	5	17	14	53	2	0	97	45.4
HC	3	2	0	3	32	16	3	1874	0	1933	3.1
NAW	0	0	0	0	0	1	0	0	109	110	0.9
Total	659	836	70	92	620	371	75	1915	109	4747	
Commission error (%)	13.7	9.4	28.6	42.4	31.9	23.2	29.3	2.1	0.0		

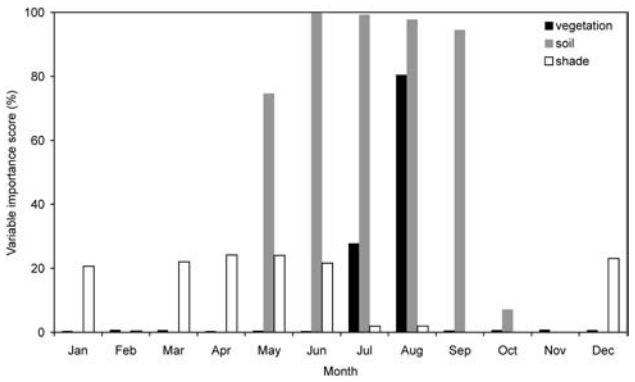

Figure 5. Diagram of CART variable importance score of the probability bagging classification tree built from the filtered training dataset. The scores are averages of the individual 25 sub-classifiers.

The land-cover map for Mato Grosso generated with the probability bagging classifier in shown in Plate 1. The BEF class is concentrated mainly in the northwest part of the state, and the SEF class in the northeast region, primarily along the Xingu river. The SDF class occurs in a small area, mainly located in the northern part of the state. *Cerrado* savanna classes, concentrated in the southern and eastern regions of Mato Grosso, are strongly dominated by BEST, followed by BES, BEW, and OG. Some of the areas with BES are located in seasonally flooded regions, namely those around the Araguaia river (eastern Mato Grosso) and the Pantanal (southern Mato Grosso). Areas under agriculture or pasture use (HC) represent the major land-cover type in Mato Grosso, with 271,768 km^2. Assuming that agriculture and pasture use in 2000 corresponds to areas that were deforested in the past, then our estimate is much higher than the 143,930 km^2 provided by INPE (2002), and close to the 270,283 km^2 estimated by FEMA-MT by the end of 1999 (SEPLAN, 2002). The difference is the consequence that our study and FEMA-MT considered deforestation in areas of *cerrado* savanna, which was not the case of INPE. This numbers indicate that deforestation in regions of *cerrado* savanna has been as intense as in areas of ombrophyllous and seasonal forest.

Accuracy Assessment and Comparison with Existing Maps

The application of the probability bagging classification tree yielded the possibility of constructing maps of probability-based rankings of class membership, i.e., spatial representation of classification membership associated with each pixel (Figure 6). Over 75 percent of the study area has a class membership greater than 0.6, and approximately 60 percent of the area has class membership greater than 0.8. Higher-class membership values are associated with HC, NAW, BEF, and SEF classes, which is emphasized by comparing class membership with class-specific commission errors (Figure 7).

These results agree with the findings of McIver and Friedl (2001), that traditional class-specific errors are strongly inversely correlated with mean probability of class membership. These results also show that discrimination between *cerrado* savanna classes (BEW, BEST, BES, and OG) is difficult. The poor spectral separability between these classes and the spatial resolution of the VGT sensor possibly

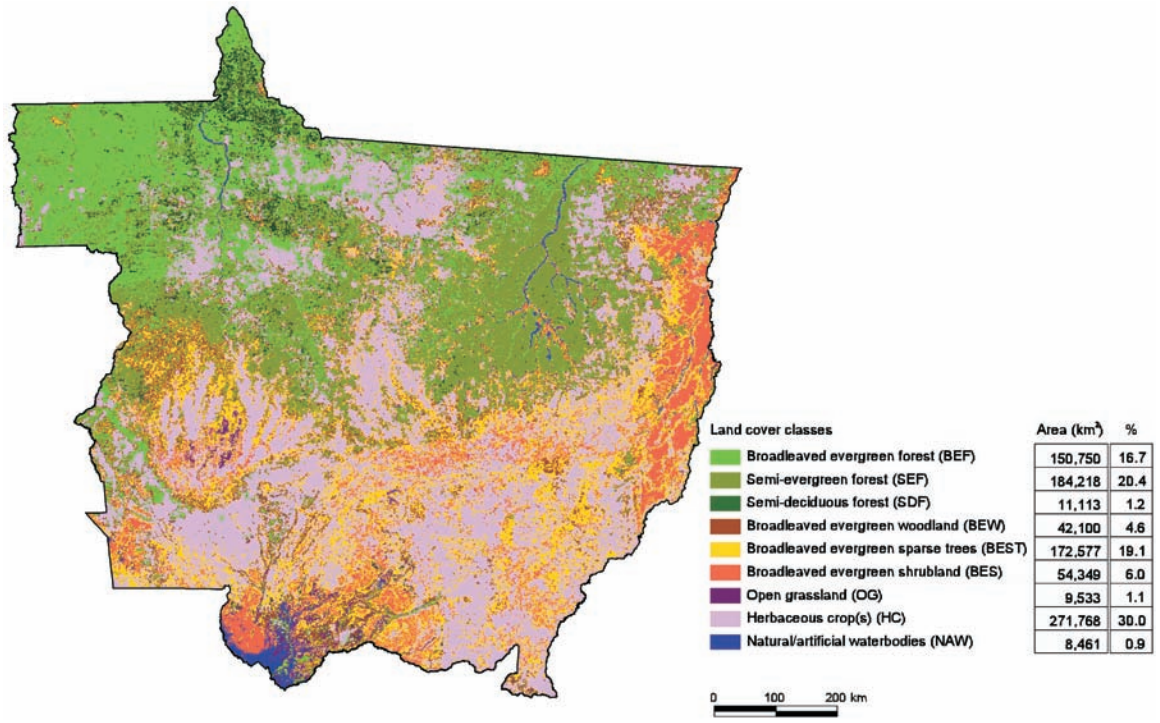

Plate 1. Land-cover map of the state of Mato Grosso, Brazil, for the year 2000, derived from the probability bagging classification tree built from the filtered training dataset. The table indicates the total area (km^2) and percentage occupied by each land-cover class.

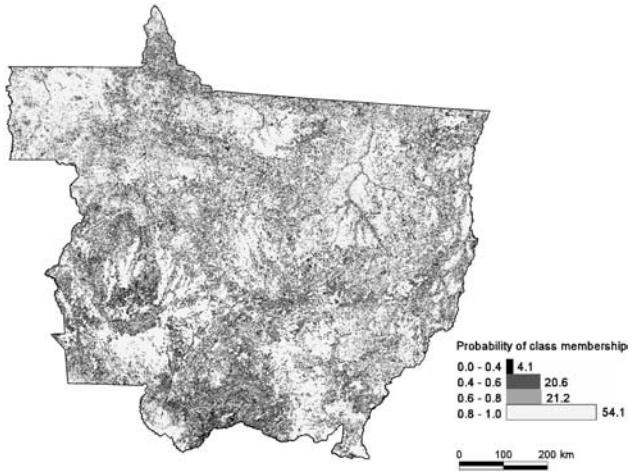

Figure 6. Classification membership map for the state of Mato Grosso derived from the probability bagging classification tree built with the filtered training dataset. Each bar represents the color scheme used and the size is proportional to the presence of each class of classification membership (it is also represented the respective percentage).

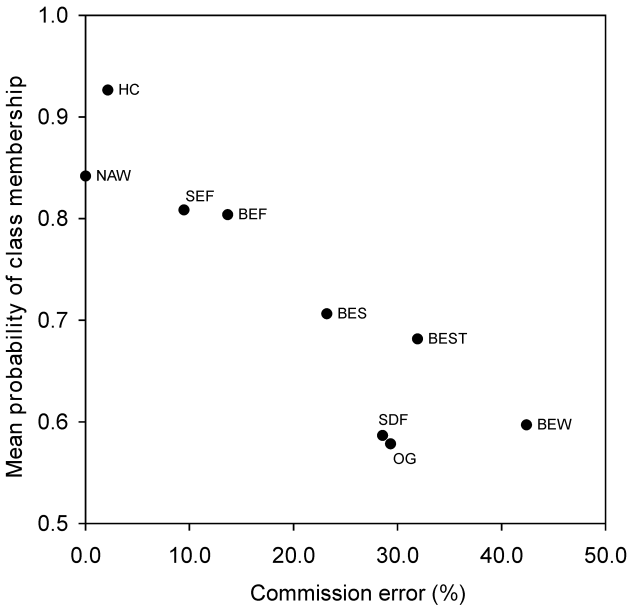

Figure 7. Comparison between mean class membership probability and class-specific commission errors.

explains this outcome. Similar comments apply to the SDF class, which also has low mean probability of class membership. Overall mean map probability of class membership is 0.80, which is lower than the classifier overall accuracy (0.88). Considering that classifier accuracy generally overestimates map accuracy (Smits *et al.*, 1999; Foody, 2002), the underestimation indicated by the overall mean map probability of class membership suggests that this measure possibly is a more rigorous estimator of map accuracy.

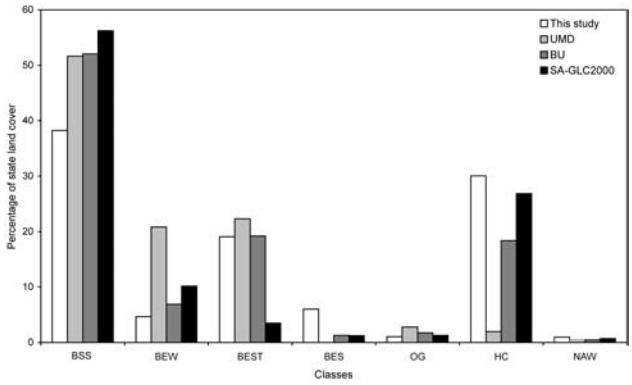

Figure 8. Comparison of estimates of class extent in the state of Mato Grosso, derived from this study, and from the UMD (Hansen *et al.*, 2000), BU (Friedl *et al.*, 2002), and SA-GLC2000 (Eva *et al.*, 2002) land-cover maps. The BSS class results from the aggregation of the BEF, SEF, and SDF classes.

Comparison with existing land-cover maps is another useful way of evaluating the land-cover map created in this study. Figure 8 compares the extent of the land-cover classes derived from this study and from the UMD, BU, and SA-GLC2000 land-cover maps. The UMD land-cover map reflects the fact that the data used are from early 1990s. Thus, the extent of the HC class is much lower than that estimated in this study, and, consequently, the aggregated BSS and *cerrado* savanna classes extents are much higher in the UMD dataset, the exception being the BES class; some discrepancies in the *cerrado* savanna classes could result from differences in legend comparison, because these transition land-cover types are more likely to be classified differently in the various land cover classes. In the BU land-cover map, the percentage occupied by the aggregated BSS class is much higher than that estimated in this study, but conversely the HC class percentage is much lower; percentage of *cerrado* savanna classes are similar, the exception being the BES class. The SA-GLC2000 land-cover map was partially derived from the same data we used and following a similar legend approach; the percentage of HC class is very similar, and the main difference occurs in the aggregated BSS class and in some *cerrado* savanna classes (BEST and BES); the type of classification algorithm used (unsupervised isodata) can explain that difference. The global overall accuracy of the UMD land-cover map was 0.69 (Hansen *et al.*, 2000). The BU dataset provides also maps of classification confidence, similar to the one used in this study, and overall mean class confidence for the state of Mato Grosso was 0.77 (Friedl *et al.*, 2002), very close to our estimate (0.80). Currently there is no extensive information about accuracy for the SA-GLC2000 map.

Data from the SPOT-4 VGT Global Burnt Area 2000 (GBA2000) Project led by the Joint Research Center (JRC) of the European Union indicates that during the year 2000 the area burnt in Mato Grosso was 7,626 km^2, mainly concentrated in the UMD dataset regions of *cerrado* savanna (Tansey *et al.*, 2004). Combination of the GBA2000 dataset with our land cover map indicates that burnt areas were mapped mainly (over 90 percent) as *cerrado* savanna classes. These fires are predominantly set by farmers to promote pasture renewal and to clear fields for cultivation (Coutinho, 1990). This low value of area burned can be explained by the fact

that the year 2000 was a La Niña year, characterized by unusually cool temperatures in the equatorial Pacific Ocean (Tansey *et al.*, 2004). The relatively small extent of area burned in Mato Grosso suggests little influence in classification results derived from our study.

Conclusions

This study concluded that vegetation and soil fraction images from dry season months were more important for land-cover classification in the state of Mato Grosso than variables from the wet season. Conversely, it appeared that shade fraction images had less influence in discriminating land-cover classes. Identification of mislabelled training data in a classification tree approach effectively increased overall and class-specific accuracy for simple and probability bagging classification trees. The concomitant use of filtering and probability bagging produced the highest overall and class-specific accuracy. Nevertheless, semi-deciduous forest and *cerrado* savanna classes still presented high classification errors, but derived from misclassification with spectrally similar classes. Additionally, the use of probability-based rankings of class membership derived from probability bagging classification trees played an important role, as maps of classification membership provided additional information for assessing map accuracy. The importance of producing both a land-cover map and a classification confidence (membership) map has also been emphasized by McIver and Friedl (2001), Friedl *et al.* (2002), and Liu *et al.* (2004). The quantification of classification confidence on a pixel-by-pixel basis can, probably, support a more complete assessment of land-cover maps for studies of regional to global land-cover monitoring. The discrepancies between this study and the available land-cover maps suggest that additional improvements are required for land-cover mapping from remote sensing data, namely the creation of structured procedures for legend definition, organizing/updating a broad network of reference land-cover types, and the obligatoriness of classification confidence/membership maps.

This study demonstrated the usefulness of the 1 km low-resolution SPOT VEGETATION imagery in classifying land cover in the state of Mato Grosso, Brazil, for the year 2000. Future work will concentrate on the development of a land-cover map for the entire Brazilian Amazon, with special focus on agriculture/pasture and secondary succession forest classes.

Acknowledgments

The authors gratefully acknowledge the three anonymous reviewers for their helpful comments and suggestions. João M. B. Carreiras work was partially developed at Instituto Nacional de Pesquisas Espaciais (INPE, Brazil), as a contribution to the Global Land-cover 2000 (GLC2000) project and to the Large Scale Biosphere-Atmosphere Experiment in Amazonia (LBA). This work was funded by a doctoral grant from the Ministério da Ciência e Tecnologia, Fundação para a Ciência e a Tecnologia, Portugal (Reference PRAXIS XXI/BD/21507/99). VEGETATION images were obtained in the framework of the GLC2000 and GBA2000 projects of the Joint Research Centre (JRC, European Commission).

References

Achard, F., H.D. Eva, and P. Mayaux, 2001. Tropical forest mapping from coarse spatial resolution satellite data: production and accuracy assessment issues, *International Journal of Remote Sensing*, 22(14):2741–2762.

Adams, J.B., M.O. Smith, and P.E. Johnson, 1986. Spectral mixture modelling: a new analysis of rock and soil types at the Viking Lander 1 site, *Journal of Geophysical Research*, 91(B8):8098–8112.

Adams, J.B., D.E. Sabol, V. Kapos, R. Almeida Filho, D.A. Roberts, M.O. Smith, and A.R. Gillespie, 1995. Classification of multispectral images based on fractions of endmembers: Application to land-cover change in the Brazilian Amazon, *Remote Sensing of Environment*, 52(2):137–154.

Aguiar, A.P.D., Y.E. Shimabukuro, and N.D.A. Mascarenhas, 1999. Use of synthetic bands derived from mixing models in the multispectral classification of remote sensing images, *International Journal of Remote Sensing*, 20(4):647–657.

Batjes, N.H., and W.G. Sombroek, 1997. Possibilities for carbon sequestration in tropical and subtropical soils, *Global Change Biology*, 3(2):161–173.

Bauer, E., and R. Kohavi, 1998. An empirical comparison of voting classification algorithms: Bagging, boosting, and variants, *Machine Learning*, 36(1/2):105–142.

Bell, J.F., 1996. Application of classification trees to the habitat preference of upland birds, *Journal of Applied Statistics*, 23(2/3):349–359.

Boardman, J.W., 1993. Automating spectral unmixing of AVIRIS data using convex geometry concepts, *Summaries of the Fourth Annual JPL Airborne Geoscience Workshop*, 25–29 October, Arlington, Virginia (JPL Pub. 93–26, Pasadena, California), pp. 11–14.

Boardman, J.W., F.A. Kruse, and R.O. Green, 1995. Mapping target signatures via partial unmixing of AVIRIS data, *Summaries of the Fifth JPL Airborne Earth Science Workshop*, 23–26 January, Washington, D.C. (JPL Pub. 95–1, Pasadena, California), pp. 23–26.

Brazil, 1980. *RADAMBRASIL, Folha SC. 21 – Juruena. Geologia, geomorfologia, pedologia, vegetação e uso potencial da terra (Levantamento dos Recursos Naturais, v.20)*, Departamento Nacional de Produção Mineral, Rio de Janeiro, Brazil, 456 p.

Brazil, 1982a. *RADAMBRASIL, Folha SD. 21 – Cuiabá. Geologia, geomorfologia, pedologia, vegetação e uso potencial da terra (Levantamento dos Recursos Naturais, v.26)*, Departamento Nacional de Produção Mineral, Rio de Janeiro, Brazil, 540 p.

Brazil, 1982b. *RADAMBRASIL, Folha SE. 21 – Corumbá. Geologia, geomorfologia, pedologia, vegetação e uso potencial da terra (Levantamento dos Recursos Naturais, v.27)*, Departamento Nacional de Produção Mineral, Rio de Janeiro, Brazil, 448 p.

Breiman, L., J. Friedman, R. Olshen, and C. Stone, 1984. *Classification and Regression Trees*, Wadsworth, Pacific Grove, California, 126 p.

Breiman, L., 1996. Bagging predictors, *Machine Learning*, 24(2): 123–140.

Breiman, L., 1998. Arcing classifiers, *The Annals of Statistics*, 26(3): 801–849.

Brodley, C.E., and M.A. Friedl, 1996. Identifying and eliminating mislabeled training instances, *Proceedings of the Thirteenth National Conference on Artificial Intelligence*, 4–8 August 1999, Portland, Oregon (American Association for Artificial Intelligence Press, Menlo Park, California), pp. 799–805.

Brodley, C.E., and M.A. Friedl, 1999. Identifying mislabeled training data, *Journal of Artificial Intelligence Research*, 11:131–167.

Brown de Colstoun, E.C., M.H. Story, C. Thompson, K. Commisso, T.G. Smith, and J.R. Irons, 2003. National Park vegetation mapping using multitemporal Landsat/data and a decision tree classifier, *Remote Sensing of Environment*, 85(3):316–327.

Bruno, F., D. Cocchi, and C. Trivisano, 2004. Forecasting daily high ozone concentrations by classification trees, *Environmetrics*, 15(2):141–153.

Cardille, J.A., and J.A. Foley, 2003. Agricultural land-use change in Brazilian Amazônia between 1980 and 1995: Evidence from integrated satellite and census data, *Remote Sensing of Environment*, 87(4):551–562.

Carreiras, J.M.B., Y.E. Shimabukuro, and J.M.C. Pereira, 2002. Fraction images derived from SPOT-4 VEGETATION data to assess land-cover change over the state of Mato Grosso, Brazil, *International Journal of Remote Sensing*, 23(23):4979–4983.

Carreiras, J.M.B., and J.M.C. Pereira, 2005. SPOT-4 VEGETATION multi-temporal compositing for land-cover change studies over

tropical regions, *International Journal of Remote Sensing*, 26(7):1323–1346.

Chang, C.-I., and D.C. Heinz, 2000. Constrained subpixel target detection for remotely sensed imagery, *IEEE Transactions on Geoscience and Remote Sensing*, 38(3):1144–1159.

Cochrane, M.A., and C.M. Souza Jr, 1998. Linear mixture model classification of burned forests in the Eastern Amazon, *International Journal of Remote Sensing*, 19(17):3433–3440.

Congalton, R.G., 1988. Using spatial autocorrelation analysis to explore the errors in maps generated from remotely sensed data, *Photogrammetric Engineering & Remote Sensing*, 54(5):587–592.

Congalton, R.G., 1991. A review of assessing the accuracy of classifications of remotely sensed data, *Remote Sensing of Environment*, 37(1):35–46.

Congalton, R.G., 2001. Accuracy assessment and validation of remotely sensed and other spatial information, *International Journal of Wildland Fire*, 10(3/4):321–328.

Coutinho, L.M., 1990. Fire in the ecology of the Brazilian cerrado, *Fire in the Tropical Biota – Ecosystem Processes and Global Challenges* (J.G. Goldhammer, editor), Springer-Verlag, Berlin, pp. 82–105.

Cross, A.M., J.J. Settle, N.A. Drake, and R.T.M. Paivinen, 1991. Subpixel measurement of tropical forest cover using AVHRR data, *International Journal of Remote Sensing*, 12(5):1119–1129.

DeFries, R.S., M. Hansen, J.R.G. Townshend, and R. Sohlberg, 1998. Global land-cover classification at 8 km spatial resolution: the use of training data derived from Landsat imagery in decision tree classifiers, *International Journal of Remote Sensing*, 19(16): 3141–3168.

DeFries, R.S., and J.C.-W. Chan, 2000. Multiple criteria for evaluating machine learning algorithms for land-cover classification from satellite data, *Remote Sensing of Environment*, 74(3): 503–515.

Di Gregorio, A., and L.J.M. Jansen, 2000. *Land-cover Classification System – LCCS. Classification Concepts and User Manual*, Food and Agriculture Organization of the United Nations, Rome, 179 p.

Eva, H.D., A.S. Belward, E.E. De Miranda, C.M. Di Bella, V. Gonds, O. Huber, S. Jones, M. Sgrenzaroli, and S. Fritz, 2004. A land-cover map of South America, *Global Change Biology*, 10(5): 731–744.

Fearnside, P.M., 1993. Deforestation in Brazilian Amazonia: The effect of population and land tenure, *Ambio*, 22(8):537–545.

Fearnside, P.M., 2003. Deforestation control in Mato Grosso: A new model for slowing the loss of Brazil's Amazon forest, *Ambio*, 32(5):343–345.

Fearnside, P.M., and R.I. Barbosa, 2003. Avoided deforestation in Amazonia as a global warming mitigation measure: The case of Mato Grosso, *World Resource Review*, 15(3):352–361.

Foody, G.M., 1999. The continuum of classification fuzziness, *Photogrammetric Engineering & Remote Sensing*, 65(4):443–451.

Foody, G.M., 2002. Status of land-cover classification accuracy assessment, *Remote Sensing of Environment*, 80(1):185–201.

Franco-Lopez, H., A.R. Ek, and M.E. Bauer, 2001. Estimation and mapping of forest stand density, volume, and cover type using the *k*-nearest neighbors method, *Remote Sensing of Environment*, 77(3):251–274.

Freund, Y., and R. Schapire, 1996. Experiments with a new boosting algorithm, *Proceedings of the Thirteenth International Conference on Machine Learning*, (Morgan Kaufmann and L. Saitta, editors), 03–06 July, Bari, pp. 148–156.

Friedl, M.A., and C.E. Brodley, 1997. Decision tree classification of land-cover from remotely sensed data, *Remote Sensing of Environment*, 61(3):399–409.

Friedl, M.A., C.E. Brodley, and A.H. Strahler, 1999. Maximizing land-cover classification accuracies produced by decision trees at continental to global scales, *IEEE Transactions on Geoscience and Remote Sensing*, 37(2):969–977.

Friedl, M.A., C. Woodcock, S. Gopal, D. Muchoney, A.H. Strahler, and C. Barker-Schaaf, 2000. A note on procedures used for accuracy assessment in land-cover maps derived from AVHRR data, *International Journal of Remote Sensing*, 21(5):1073–1077.

Friedl, M.A., D.K. McIver, J.C.F. Hodges, X.Y. Zhang, D. Muchoney, A.H. Strahler, C.E. Woodcock, S. Gopal, A. Schneider, A. Cooper, A. Baccini, F. Gao, and C. Schaaf, 2002. Global land-cover mapping from MODIS: algorithms and early results, *Remote Sensing of Environment*, 83(1/2):287–302.

Friedman, J., T. Hastie, and R. Tibshirani, 2000. Additive logistic regression: A statistical view of boosting, *The Annals of Statistics*, 28(2):337–407.

Goulding, M., R. Barthem, and E. Ferreira, 2003. *The Smithsonian Atlas of the Amazon*, Smithsonian Books, Washington, D.C., 256 p.

Green, A.A., M. Berman, P. Switzer, and M.D. Craig, 1988. A transformation for ordering multispectral data in terms of image quality with implications for noise removal, *IEEE Transactions on Geoscience and Remote Sensing*, 26(1):65–74.

Hansen, M., R. Dubayah, and R. DeFries, 1996. Classification trees: An alternative to traditional land-cover classifiers, *International Journal of Remote Sensing*, 17(5):1075–1082.

Hansen, M., R. DeFries, J.R.G. Townshend, and R. Sohlberg, 2000. Global land-cover classification at 1 km resolution using a decision tree classifier, *International Journal of Remote Sensing*, 21(6/7):1331–1364.

Holben, B.N., and Y.E. Shimabukuro, 1993. Linear mixing model applied to coarse spatial resolution data from multispectral satellite sensors, *International Journal of Remote Sensing*, 14(11):2231–2240.

Houghton, R.A., 2000. Interannual variability in the global carbon cycle, *Journal of Geophysical Research*, 105(D15):20121–20130.

Houghton, R.A., D.L. Skole, C.A. Nobre, J.L. Hackler, K.T. Lawrence, and W.H. Chomentowski, 2000. Annual fluxes of carbon from deforestation and regrowth in the Brazilian Amazon, *Nature*, 403:301–304.

Houghton, R.A., K.T. Lawrence, J.L. Hackler, and S. Brown, 2001. The spatial distribution of forest biomass in the Brazilian Amazon: a comparison of estimates, *Global Change Biology*, 7(7):731–746.

Huete, A.R., 1988. A soil-adjusted vegetation index (SAVI), *Remote Sensing of Environment*, 25(3):295–309.

Ichoku, C., and A. Karnieli, 1996. A review of mixture modelling techniques for sub-pixel land-cover estimation, *Remote Sensing Reviews*, 13:161–186.

IBGE, 2000. *Atlas Nacional do Brasil*, Instituto Brasileiro de Geografia e Estatística, Rio de Janeiro, Brazil, 262 p.

INPE, 2002. *Monitoring of the Brazilian Amazonian forest by satellite – 2000–2001*, Instituto Nacional de Pesquisas Espaciais, São José dos Campos, SP, Brazil, 21 p.

INPE, 2005. Monitoramento da floresta amazônica brasileira por satélite. Projeto Prodes, Coordenação-Geral de Observação da Terra, Instituto Nacional de Pesquisas Espaciais, São José dos Campos, SP, Brazil URL: http://www.obt.inpe.br/prodes/, (last date accessed: 12 May 2006).

John, G.H., 1995. Robust decision trees: Removing outliers from databases, *Proceedings of the First International Conference on Knowledge Discovery and Data Mining* (U.M. Fayyad and R. Uthurusamy, editors) 20–21 August, Montreal (American Association for Artificial Intelligence Press, Menlo Park, California, pp. 174–179.

Kaimowitz, D., and J. Smith, 2001. Soybean technology and the loss of natural vegetation in Brazil and Bolivia, *Agricultural Technologies and Tropical Deforestation* (A. Angelsen and D. Kaimowitz, editors), CAB International Publishing, Oxon, U.K., pp. 195–211.

Lambin, E.F., H.J. Geist, and E. Lepers, 2003. Dynamics of land-use and land-cover change in tropical regions, *Annual Review of Environment and Resources*, 28:205–241.

Lillesand, T.M., and R.W. Kiefer, 1994. *Remote Sensing and Image Interpretation*, John Wiley & Sons, New York, 750 p.

Liu, W.G., S. Gopal, and C.E. Woodcock, 2004. Uncertainty and confidence in land-cover classification using a hybrid classifier approach, *Photogrammetric Engineering & Remote Sensing*, 70(8):963–971.

Lu, D., E. Moran, and M. Batistella, 2003. Linear mixture model applied to Amazonian vegetation classification, *Remote Sensing of Environment*, 87(4):456–469.

Maclin, R., and D. Opitz, 1997. An empirical evaluation of bagging and boosting, *Proceedings of the Fourteenth National Conference on Artificial Intelligence*, 27–31 July, Providence, Rhode Island (American Association for Artificial Intelligence Press, Menlo Park, California), pp. 546–551.

McIver, D.K., and M.A. Friedl, 2001. Estimating pixel-scale land-cover classification confidence using nonparametric machine learning methods, *IEEE Transactions on Geoscience and Remote Sensing*, 39(9):1959–1968.

McIver, D.K., and M.A. Friedl, 2002. Using prior probabilities in decision-tree classification of remotely sensed data, *Remote Sensing of Environment*, 81(2/3):253–261.

Miranda, A.C., H.S. Miranda, J. Lloyd, J. Grace, J.A. McIntyre, P. Meir, P. Riggan, R. Lockwood, and J. Brass, 1996. Carbon dioxide fluxes over a cerrado *sensu stricto* in central Brazil, *Amazonian Deforestation and Climate* (J.H.C. Gash, C.A. Nobre, J.M. Roberts, and R.L. Victoria, editors), John Wiley and Sons, Chichester, U.K., pp. 353–363.

Moran, E.F., 1993. Deforestation and land-use in the Brazilian Amazon, *Human Ecology*, 21(1):1–21.

Moran, E.F., E. Brondizio, P. Mausel, and Y. Wu, 1994. Integrating Amazonian vegetation, land-use, and satellite data, *Bioscience*, 44(5):329–338.

Muchoney, D.M., and A.H. Strahler, 2002. Pixel- and site-based calibration and validation methods for evaluating supervised classification of remotely sensed data, *Remote Sensing of Environment*, 81(2/3):290–299.

Nepstad, D.C., C.A. Klink, C. Uhl, I.C. Vieira, P. Lefebvre, M. Pedlowski, E. Matricardi, G. Negreiros, I.F. Brown, E. Amaral, A. Homma, and R. Walker, 1997. Land-use in Amazonia and the Cerrado of Brazil, *Ciência e Cultura Journal of the Brazilian Association for the Advancement of Science*, 49(1/2): 73–86.

Oleson, K.W., S. Sarlin, J. Garrison, S. Smith, J.L. Privette, W.J. Emery, 1995. Unmixing multiple land-cover type reflectances from coarse spatial resolution satellite data, *Remote Sensing of Environment*, 54(2):98–12.

Passot, X., 2000. VEGETATION image processing methods in the CTIV, *Proceedings of VEGETATION 2000–2 Years of Operation to Prepare the Future*, 03–06 April, Ispra, Italy, (SAI/JRC, Ispra, Italy), pp. 15–21.

Perlich, C., F. Provost, and J.S. Simonoff, 2003. Tree induction vs. logistic regression: A learning-curve analysis, *Journal of Machine Learning Research*, 4:211–255.

Provost, F., and P. Domingos, 2003. Tree induction for probability-based ranking, *Machine Learning*, 52(3):199–215.

Quarmby, N.A, J.R.G. Townshend, J.J. Settle, K.H. White, M. Milnes, T.L. Hindle, and N. Silleos, 1992. Linear mixture modeling applied to AVHRR data for crop area estimation, *International Journal of Remote Sensing*, 13(3):415–425.

Research Systems, Inc., 2000. *ENVI version 3.4 – User's Guide*, Research Systems, Boulder, Colorado, 930 p.

Richards, J.A., 1986. *Remote Sensing Digital Image Analysis*, Springer-Verlag, Berlin, 291 p.

Rodríguez-Yi, J.L., Y.E. Shimabukuro, and B.F.T. Rudorff, 2000. Image segmentation for classification of vegetation using NOAA AVHRR data, *International Journal of Remote Sensing*, 21(1): 167–172.

Safavian, S.R., and D. Landgrebe, 1991. A survey of decision tree classifier methodology, *IEEE Transactions on Systems, Man, and Cybernetics*, 21(3):660–674.

Schulze, E.-D., D. Mollicone, F. Achard, G. Matteucci, S. Federici, H.D. Eva, R. Valentini, 2003. Making deforestation pay under the Kyoto Protocol ?, *Science*, 299:1669.

SEPLAN, 2002. *Anuário Estatístico do Mato Grosso – 2002*, Secretaria de Estado de Planejamento e Coordenação Geral, Cuiabá, Mato Grosso, Brazil, URL: http://www.anu.seplan.mt.gov.br/index-anua2002.htm (last date accessed: 12 May 2006).

Shimabukuro, Y.E., and J.A. Smith, 1991. The least-squares mixing models to generate fraction images derived from remote sensing multispectral data, *IEEE Transactions on Geoscience and Remote Sensing*, 29(1):16–20.

Shimabukuro, Y.E., and J.A. Smith, 1995. Fraction images derived from Landsat TM and MSS data for monitoring reforested areas, *Canadian Journal of Remote Sensing*, 21(1):67–74.

Smits, P.C., S.G. Dellepiane, and R.A. Schowengerdt, 1999. Quality assessment of image classification algorithms for land-cover mapping: a review and a proposal for a cost-based approach, *International Journal of Remote Sensing*, 20(8):1461–1486.

Souza Jr., C., L. Firestone, L. Moreira Silva, and D. Roberts, 2003. Mapping forest degradation in the Eastern Amazon from SPOT 4 through spectral mixture models, *Remote Sensing of Environment*, 87(4):494–506.

Tansey, K., J-M. Grégoire, D. Stroppiana, A. Sousa, J. Silva, J. Pereira, L. Boschetti, M. Maggi, P. Brivio, R. Fraser, S. Flasse, D. Ershov, E. Binaghi D. Graetz, and P. Peduzzi, 2004. Vegetation burning in the year 2000: Global burned area estimates from SPOT VEGETATION data, *Journal of Geophysical Research*, 109, D14S03, doi:10.1029/2003JD003598.

University of Maryland, 2005. Global land-cover Facility, University of Maryland, URL: http://glcf.umiacs.umd.edu/index.shtml, (last date accessed: 12 May 2006).

Veloso, H.P., A.M.S. Japiassu, L. Goes Filho, and P.F. Leite, 1974. As regiões fitoecológicas, sua natureza e seus recursos económicos, *Projeto Radambrasil. Folha SB.22 Araguaia e parte da folha SC.22 Tocantins*, Departamento Nacional de Produção Mineral, Rio de Janeiro, Brazil, pp. 1–119.

Vitousek. P.M., H.A. Mooney, J. Lubchenco, and J.M. Melillo, 1997. Human domination of Earth's ecosystems, *Science*, 277:494–499.

(Received 07 January 2005; accepted 20 January 2005; revised 01 March 2005)